



pH-Responsive Cytotoxicity of a Magnetic Iron-Based Nanocomposite in Normal and Cancer Cell Models

A. Asanova^{1,4*}, A. Eftekhari¹, M. F. Baran², A. Baran³, M. Sultanova⁴

¹Department of Biochemistry, Faculty of Science, Ege University, Izmir, Turkiye

²Department of Food Technology, Vocational School of Technical Sciences, Batman University, Batman, Turkiye

³Department of Field Crops, Kiziltepe Faculty of Agricultural Sciences and Technologies, Mardin Artuklu University, Kiziltepe, Mardin, Turkiye

⁴Azerbaijan Medical University, Baku, Azerbaijan

nastasia.asanova@gmail.com

Abstract. pH-responsive nanocarriers with magnetic cores represent a promising approach for targeted drug delivery. Nevertheless, their potential cytotoxicity remains a concern. This study re-evaluates published data on the magnetic nanocomposite IONPs@CtAC-MR, composed of iron oxide nanoparticles, activated carbon, and the flavonoid morin, to assess its pH responsiveness and cytotoxicity. The analysis focused on its effects in human umbilical vein endothelial cells (HUVECs) and two tumor cell lines: glioblastoma (T98-G) and colorectal adenocarcinoma (HT-29). Viability was assessed via MTT assay after 24 and 48 hours of exposure to the nanocomposite at concentrations of 50, 100, and 200 µg/mL, under both physiological (pH 7.4) and acidic (pH 5.4) conditions.

HUVEC cells retained high viability (~89%) at neutral pH across all concentrations and time points but showed a decrease (~69%) under acidic conditions, independent of dose or exposure duration, suggesting sensitivity to pH-induced stress. T98-G cells proliferated at pH 7.4 (133%, 24 h, 50 µg/mL), with viability increasing at higher doses and longer exposure. Under the same conditions, acidic pH reduced viability to 51%, but it recovered to 142% at 200 µg/mL after 48 h. HT-29 cells also showed high viability under neutral pH (~137%, 24 h, 50 µg/mL) with a weak influence of concentration. However, in acidic conditions, viability declined (77%) and remained stable regardless of concentration or duration.

The relative contribution of the examined factors to cell viability can be ranked as follows: **cell line > pH > concentration > time**.

The nanocomposite exhibited favorable biocompatibility and selective cytotoxicity, supporting its potential as a pH-responsive drug delivery platform.

Keywords: pH-responsive nanocomposite; magnetic nanoparticles; cytotoxicity.

1 Introduction

Nanotechnology has revolutionized numerous fields, including medicine, due to the unique physicochemical properties of nanomaterials. Among the most promising applications is their use in targeted drug delivery systems, which offer increased therapeutic precision and reduced systemic side effects [1]. Incorporating a magnetic core into such systems enables external magnetic field-guided transport of therapeutic agents, facilitating localized drug accumulation at the site of interest [2, 3]. This strategy significantly improves therapeutic efficacy while minimizing off-target toxicity.

Effective drug delivery design must consider not only physical targeting mechanisms but also the distinct features of pathological microenvironments. A key hallmark of many solid tumors is extracellular acidosis, with local pH levels significantly lower than those in normal tissues. Consequently, the development of nanocarriers capable of releasing their payloads selectively in acidic environments is a highly relevant approach in anticancer therapy.

However, concerns remain regarding the potential cytotoxicity of magnetic nanoparticles, particularly those based on iron oxides [1, 4]. These particles may release free iron ions or generate reactive oxygen species, leading to oxidative stress and cellular damage. To enhance biocompatibility and minimize adverse interactions with biological systems, carbon-based surface coatings have been widely investigated. In this study, we used a previously developed nanocomposite (IONPs@CtAC-MR), consisting of iron oxide nanoparticles coated with activated carbon and loaded with morin hydrate [5,6].

Morin (3,5,7,2',4'-pentahydroxyflavone), a naturally occurring flavonoid, has been extensively studied for its anti-inflammatory, antioxidant, hepatoprotective, antidiabetic, and anticancer properties [7,8].

The aim of this study was to evaluate the pH-dependent cytotoxicity of IONPs@CtAC-MR in human endothelial cells (HUVEC) and two tumor-derived lines (T98-G glioblastoma and HT-29 colorectal adenocarcinoma) across different concentrations and incubation times. Building on prior experimental work [6], we conducted an independent statistical reanalysis of the published cell-viability dataset to explore potential pH-related and multifactorial dependencies, such as the combined influence of acidity, concentration, and exposure time.

2 Materials and methods

The IONPs@CtAC-MR nanocomposite used in this study was synthesized and characterized previously by Öziç et al. [5] and Doğan et al. [6]. It consists of superparamagnetic Fe₃O₄ nanoparticles coated with activated carbon derived from *Celtis tournefortii* and loaded with morin. Structural analysis confirmed a cubic spinel phase with an average crystallite size of 24.8 nm, a hydrodynamic particle size of approximately 164.2 nm, saturation magnetization of 66.41 emu/g, and a zeta potential of -15.9 mV, indicative of good colloidal stability [5,6].

cell viability data were obtained from previously published experiments by Doğan et al. [6], who investigated the cytotoxic effects of IONPs@CtAC-MR on human umbilical vein endothelial cells (HUVEC), glioblastoma cells (T98-G), and colorectal adenocarcinoma cells (HT-29). Cells were cultured under standard conditions (37 °C, 5% CO₂) and seeded at a density of 1×10^5 cells/well in 96-well plates, following the culture conditions originally adapted from Baran et al. [9].

Cells were treated with IONPs@CtAC-MR at concentrations of 50, 100, and 200 µg/mL. Treatments were carried out in phosphate-buffered saline (PBS) adjusted to two pH values: 7.4 (physiological) and 5.4 (tumor-mimicking acidic microenvironment). Incubation periods were 24 and 48 h.

Cell viability was assessed using the MTT assay. Following exposure, 10 µL of MTT solution (5 mg/mL) was added to each well, and the plates were incubated for 3 h at 37 °C. After incubation, the supernatant was removed and 100 µL of DMSO was added to dissolve the formazan crystals. The plates were agitated for 20 min, and absorbance was measured at 570 nm using a MultiScan Go spectrophotometer (Thermo Scientific).

Cell viability (%) was calculated according to the following equation:

$$\text{Viability (\%)} = \left(\frac{\text{OD}_{\text{sample}}}{\text{OD}_{\text{control}}} \right) \times 100 \quad (1)$$

An independent statistical reanalysis of the original data was performed using Python. Multifactorial analysis of variance (ANOVA) was applied to determine the individual and interactive effects of pH, concentration, and exposure time. Statistical significance was defined as $p < 0.05$ ($n = 4$). Principal component analysis (PCA) was also used to explore the variance structure and identify dominant response patterns among cell lines.

3 Results and Discussion

To evaluate the biocompatibility and pH responsiveness of the IONPs@CtAC-MR nanocomposite, cell viability data for HUVEC, T98-G, and HT-29 cells were analyzed using multifactorial statistical methods. The analysis focused on how extracellular acidity, nanocomposite concentration, and exposure time interact to shape cellular responses. This approach allowed detection of subtle, non-linear patterns that may remain obscured in single-factor evaluations.

The viability of human umbilical vein endothelial cells (HUVEC) remained consistently high under physiological pH 7.4, confirming the biocompatibility of IONPs@CtAC-MR. After 24 h, viability reached $85.47 \pm 9.30\%$, $91.12 \pm 2.67\%$, and $90.08 \pm 3.74\%$ at 50, 100, and 200 µg/mL, respectively, and showed comparable values after 48 h ($92.82 \pm 8.02\%$, $88.00 \pm 2.58\%$, and $86.74 \pm 7.17\%$). Neither concentration

nor incubation time produced statistically significant effects ($p > 0.05$), indicating stable tolerance of the nanocomposite at neutral pH.

In contrast, at pH 5.4, mimicking the tumor microenvironment, cell viability markedly declined ($p < 0.0001$) across all concentrations, dropping to $74.00 \pm 2.68\%$, $65.43 \pm 5.80\%$, and $67.46 \pm 4.38\%$ after 24 h and remaining at $73.51 \pm 5.36\%$, $66.78 \pm 8.94\%$, and $65.65 \pm 7.92\%$ after 48 h. No additional time-dependent decrease was observed ($p > 0.05$).

Two-way ANOVA confirmed a pronounced main effect of pH ($p < 0.05$) without significant pH \times concentration or pH \times time interactions, emphasizing that extracellular acidity, rather than nanocomposite dose or exposure duration, is the dominant factor determining endothelial cell response. The data suggest a threshold-type effect in which acid-induced destabilization of membrane integrity and oxidative stress surpass intrinsic cellular defense capacity.

Unlike normal endothelial HUVECs, T98-G glioblastoma cells demonstrated a pronounced proliferative response under physiological conditions (pH 7.4). After 24 hours of exposure to IONPs@CtAC-MR, cell viability significantly exceeded control levels across all tested concentrations, reaching $133.27 \pm 9.69\%$, $141.15 \pm 12.10\%$, and $156.20 \pm 12.50\%$ for 50, 100, and 200 $\mu\text{g/mL}$, respectively, with higher concentrations correlating with increased viability. This effect was further enhanced after 48 hours ($p < 0.001$), with viability rising to $197.31 \pm 57.31\%$, $211.32 \pm 65.96\%$, and $216.68 \pm 87.44\%$. These results underscore the high proliferative potential and stress resistance characteristic of glioblastoma cells under favorable, non-acidic conditions.

At acidic pH (5.4), cell viability after 24 hours dropped significantly ($p < 0.001$), reaching $50.72 \pm 3.70\%$ (50 $\mu\text{g/mL}$), $78.64 \pm 20.43\%$ (100 $\mu\text{g/mL}$), and $94.25 \pm 4.53\%$ (200 $\mu\text{g/mL}$). Over time, a concentration-dependent recovery in viability was observed, suggesting a delayed proliferative response potentially mediated by morin. After 48 hours, viability significantly increased to $73.46 \pm 11.17\%$, $120.04 \pm 7.44\%$, and $141.76 \pm 3.49\%$ ($p < 0.0001$).

This biphasic pattern, initial suppression followed by recovery, demonstrates the capacity of aggressive tumor cells to adapt through metabolic reprogramming and activation of survival pathways. The concentration-dependent increase in viability under acidic stress supports the hypothesis that morin elicits a compensatory proliferative effect, likely mediated by its antioxidant and signaling-modulating properties. The widening variability across concentrations may further reflect heterogeneity in stress adaptation mechanisms.

Two-way ANOVA confirmed a multifactorial response: both pH ($p < 0.05$) and concentration ($p < 0.01$) significantly influenced viability, with a notable pH \times

concentration interaction ($p < 0.05$). In the $\text{pH} \times \text{time}$ model, the interaction term also reached significance ($p < 0.05$), indicating that T98-G cells respond synergistically to extracellular acidity, nanocomposite concentration, and exposure duration, consistent with their high metabolic activity and reduced buffering capacity.

The HT-29 colorectal adenocarcinoma cell line also exhibited pronounced proliferative activity under physiological pH 7.4. After 24 h of exposure to IONPs@CtAC-MR, cell viability significantly exceeded control levels, reaching $136.96 \pm 5.67\%$ at $50 \mu\text{g/mL}$. Increasing the concentration two- and four-fold further enhanced the proliferative response, yielding $174.56 \pm 30.83\%$ at $100 \mu\text{g/mL}$ and $176.73 \pm 19.43\%$ at $200 \mu\text{g/mL}$. Although viability increased between 50 and $100 \mu\text{g/mL}$, further dose escalation produced no statistically significant difference ($p > 0.05$), suggesting a potential saturation point in dose-dependent proliferation.

Prolonging incubation to 48 h did not result in significant changes ($p > 0.05$); viability remained consistently elevated and independent of concentration, measuring $139.97 \pm 13.55\%$, $146.54 \pm 18.69\%$, and $151.49 \pm 15.13\%$ at 50, 100, and $200 \mu\text{g/mL}$, respectively. These results indicate a sustained proliferative response of tumor cells that was unaffected by either concentration or exposure time within the tested range.

The response pattern of both tumor cell lines, T98-G glioblastoma and HT-29 colorectal adenocarcinoma, underscores the high adaptive capacity of malignant cells and their inherent tendency toward hyperproliferation under non-stressful conditions. The proliferative effect observed at pH 7.4 is consistent with the hormetic activity of morin, delivered at subcytotoxic concentrations via the nanocomposite. In tumor cells characterized by strong antioxidant defenses and metabolic plasticity, such exposure may activate growth- and survival-related signaling pathways, including Nrf2, PI3K/AKT, and MAPK, and enhance mitochondrial metabolism, ultimately promoting proliferation [7].

Under acidic conditions (pH 5.4), HT-29 cells, similar to T98-G, displayed the opposite trend. After 24 h, viability was significantly reduced to $76.88 \pm 7.32\%$, $76.62 \pm 9.59\%$, and $97.82 \pm 15.91\%$ at 50, 100, and $200 \mu\text{g/mL}$, respectively ($p < 0.0001$ vs. corresponding values at pH 7.4). After 48 h, viability remained at comparable levels, $79.90 \pm 8.74\%$, $79.90 \pm 9.01\%$, and $85.23 \pm 5.84\%$, with no statistically significant time-dependent change ($p \gg 0.05$), indicating a limited adaptive response of HT-29 cells under acidic stress.

In contrast to T98-G cells, which exhibited partial recovery over time, HT-29 cells showed no significant adaptive dynamics, suggesting a lower tolerance of colorectal tumor cells to acidosis. This sensitivity may stem from a less developed repertoire of compensatory mechanisms, reduced capacity for metabolic reprogramming, and weaker antioxidant defenses. Additionally, acidic pH may directly suppress

proliferation-related signaling active under neutral conditions while exacerbating membrane damage and ionic imbalance, thereby impairing effective stress adaptation [10].

Two-way ANOVA confirmed that HT-29 cell viability was strongly dependent on pH ($p < 0.001$) and less affected by nanocomposite concentration ($p < 0.01$), with a moderate pH \times concentration interaction ($p < 0.05$). In the pH \times time model, the interaction term was not significant ($p > 0.05$), indicating a dominant effect of medium acidity with an additional, secondary dose-dependent component.

Principal component analysis (PCA) of the experimental dataset revealed distinct clustering patterns primarily determined by medium pH and nanocomposite concentration (Fig. 1).

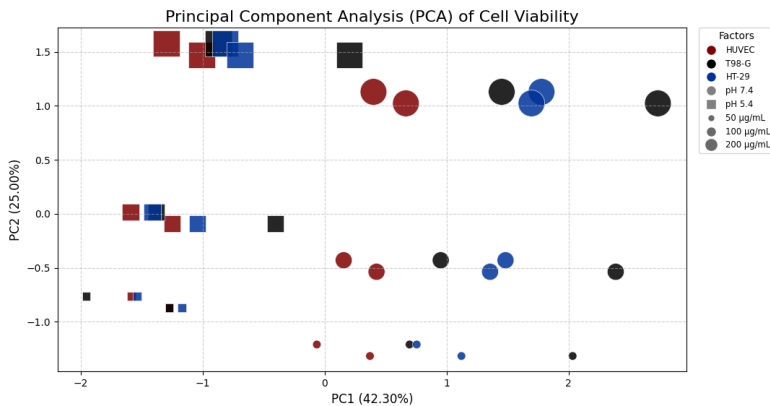


Fig. 1. Principal component analysis (PCA) of cell viability under varying four quantitative variables (pH, concentration, incubation time, and mean viability); cell line served only as a visual label and was not included in component computation.

These two variables accounted for the majority of total variance, indicating that extracellular acidity was the dominant driver of cellular responses, whereas concentration exerted secondary yet discernible effects within each pH cluster. In contrast, temporal variation was less evident on the PCA map, suggesting that exposure time contributed only modestly to the overall response profile. This pattern underscores the predominant role of extracellular acidity in modulating cellular behavior under nanoparticle exposure and is consistent with previous observations that acidic microenvironments suppress metabolic activity and proliferation even in malignant cells [11].

To compare the responses among different cell types, a multifactorial ANOVA was performed across all three cell lines. The observed decrease in viability ranked as T98-

G > HT-29 > HUVEC, reflecting the higher susceptibility of tumor-derived cells to combined acidic and nanoparticle-induced stress. This hierarchy highlights that cell-type-specific physiology and microenvironmental acidity are the principal determinants of the observed cytotoxicity patterns, whereas concentration and incubation duration act as secondary modulators of the overall cellular response.

4 Conclusion

The present findings demonstrate that extracellular pH is a critical determinant of cell viability, exerting a consistent suppressive effect across both normal (HUVEC) and malignant (HT-29, T98-G) cell lines. Under acidic conditions (pH 5.4), cellular proliferation was markedly inhibited in all models, confirming the high sensitivity of both healthy and cancerous cells to microenvironmental acidification. Importantly, the influence of pH was not isolated but interacted differently with other experimental factors. In HUVECs, no significant pH \times concentration or pH \times time interactions were detected, indicating stable tolerance under varying conditions. In contrast, T98-G glioblastoma cells exhibited strong, statistically significant interactions between pH and both concentration and exposure time, reflecting complex adaptive and proliferative dynamics. For HT-29 colorectal adenocarcinoma cells, the interaction between pH and concentration was weak yet statistically significant, while the pH \times time effect remained non-significant. These patterns collectively confirm that cytotoxicity under acidic conditions is modulated in a dose- and time-dependent manner and follows a multifactorial, non-linear response model.

Overall, the relative contribution of the studied factors can be summarized as:

Cell line > pH > concentration > time, indicating that intrinsic cellular properties exerted the strongest influence on the observed outcomes.

The IONPs@CtAC-MR nanocomposite demonstrated favorable biocompatibility and pH-dependent selectivity across all models, supporting its promise as a targeted nanotherapeutic platform. The observed differential sensitivity between normal and malignant cells suggests that such pH-responsive systems could enable selective tumor targeting while minimizing collateral effects on healthy tissues, an essential criterion for the rational design of safe and effective nanomedicines.

References

1. Islam, S., Ahmed, M.M.S., Islam, M.A., Hossain, N., & Chowdhury, M.A.: Advances in nanoparticles in targeted drug delivery—A review. *Results Surf. Interfaces* **100529** (2025). <https://doi.org/10.1016/j.rints.2024.100529>
2. Kianfar, E.: Magnetic nanoparticles in targeted drug delivery: a review. *J. Supercond. Nov. Magn.* **34**(7), 1709–1735 (2021). <https://doi.org/10.1007/s10948-021-05861-0>
3. Saikova, S.; Pavlikov, A.; Trofimova, T.; Mikhlin, Y.; Karpov, D.; Asanova, A.; Grigoriev, Y.; Volochaev, M.; Samoilo, A.; Zharkov, S., & Velikanov, D.: Hybrid nanoparticles based on cobalt ferrite and gold: preparation and characterization. *Metals* **11**(5), 705 (2021). <https://doi.org/10.3390/met11050705>

4. Nowak-Jary, J., & Machnicka, B.: Comprehensive analysis of the potential toxicity of magnetic iron oxide nanoparticles for medical applications: cellular mechanisms and systemic effects. *Int. J. Mol. Sci.* **25**(22), 12013 (2024). <https://doi.org/10.3390/ijms252212013>
5. Öziç, C., Ertaş, E., Baran, M. F., Baran, A., Ahmadian, E., Eftekhari, A., Khalilov, R., Aliyev, E., & Yıldıztekin, M.: Synthesis and characterization of activated carbon-supported magnetic nanocomposite (MNPs-OLAC) obtained from okra leaves as a nanocarrier for targeted delivery of morin hydrate. *Front. Pharmacol.* **15**, 1482130 (2024). <https://doi.org/10.3389/fphar.2024.1482130>
6. Doğan, Y., Öziç, C., Ertaş, E., Baran, A., Rosic, G., Selakovic, D., & Eftekhari, A.: Activated carbon-coated iron oxide magnetic nanocomposite (IONPs@CtAC) loaded with morin hydrate for drug-delivery applications. *Front. Chem.* **12**, 1477724 (2024). <https://doi.org/10.3389/fchem.2024.1477724>
7. Lee, M. H., Han, M. H., Lee, D.-S., Park, C., Hong, S.-H., Kim, G.-Y., Hong, S. H., Song, K. S., Choi, I.-W., Cha, H.-J., & Choi, Y.H.: Morin exerts cytoprotective effects against oxidative stress in C2C12 myoblasts via the upregulation of Nrf2-dependent HO-1 expression and the activation of the ERK pathway. *Int. J. Mol. Med.* **39**(2), 399–406 (2017). <https://doi.org/10.3892/ijmm.2016.2847>
8. Vijay, V., & Perumal, M.K.: Morin, a polypharmacological marvel: Unveiling its versatility and recent advances in bioavailability enhancement. *Food Biosci.* **59**, 106104 (2025). <https://doi.org/10.1016/j.fbio.2023.106104>
9. Baran, M.F., Keskin, C., Baran, A., Kurt, K., İpek, P., & Eftekhari, A.: Green synthesis and characterization of selenium nanoparticles (Se NPs) from the skin (testa) of *Pistacia vera* L. (Siirt pistachio) and investigation of antimicrobial and anticancer potentials. *Biomass Convers. Biorefin.* **14**, 23623–23633 (2023). <https://doi.org/10.1007/s13399-023-04366-8>
10. Zheng, Y., Sun, J., Luo, Z., Li, Y., & Huang, Y.: Emerging mechanisms of lipid peroxidation in regulated cell death and its physiological implications. *Cell Death Dis.* **15**(11), 859 (2024). <https://doi.org/10.1038/s41419-024-06813-2>
11. Ghaemi, B., Hajipour, M.J.: Tumor acidic environment directs nanoparticle impacts on cancer cells. *J. Colloid Interface Sci.* **634**, 684–692 (2023). <https://doi.org/10.1016/j.jcis.2023.05.016>

Open Access This chapter is licensed under the terms of the Creative Commons Attribution-NonCommercial 4.0 International License (<http://creativecommons.org/licenses/by-nc/4.0/>), which permits any noncommercial use, sharing, adaptation, distribution and reproduction in any medium or format, as long as you give appropriate credit to the original author(s) and the source, provide a link to the Creative Commons license and indicate if changes were made.

The images or other third party material in this chapter are included in the chapter's Creative Commons license, unless indicated otherwise in a credit line to the material. If material is not included in the chapter's Creative Commons license and your intended use is not permitted by statutory regulation or exceeds the permitted use, you will need to obtain permission directly from the copyright holder.

